DALTON
FULL PAPER

Titanium(IV)azido and imido complexes as potential precursors to titanium nitride

Claire J. Carmalt,*,†,[a] Sandra R. Whaley,[a] Pindy S. Lall,[b] Alan H. Cowley,*,[a] Richard A. Jones,[a] Brian G. McBurnett[a] and John G. Ekerdt[b]

[a] *Department of Chemistry & Biochemistry, The University of Texas at Austin, Austin, Texas 78712, USA*
[b] *Department of Chemical Engineering, The University of Texas at Austin, Austin, Texas 78712, USA*

Synthetic and structural studies have been performed for two imido complexes of titanium(IV). The reaction between $[\{Ti(NBu^t)Cl_2(NH_2Bu^t)_2\}_3]$ and 6 equivalents of Me_3SiN_3 at room temperature in the presence of pyridine resulted in the substitution of only one chloride per titanium atom and formation of the dimeric complex $[\{Ti(NBu^t)Cl(N_3)(py)_2\}_2]$ (py = pyridine). An alternative approach to such complexes, which involved the reaction between $[Ti(NMe_2)_2(N_3)_2(py)_2]$ and 1 equivalent of $CyNH_2$ at room temperature, resulted in the dimeric bis(azide) complex $[\{Ti(NCy)(N_3)_2(py)_2\}_2]$ (Cy = cyclohexyl). The two new complexes have been characterised by X-ray crystallography; the solid state of each comprises dimeric units in which the two titanium atoms are bridged by a pair of azide ligands. A gas-phase pyrolysis study has been conducted on $[Ti(NMe_2)_2(N_3)_2(py)_2]$ and preliminary CVD experiments on the two new complexes revealed that they are not effective titanium nitride precursors.

Transition-metal imido complexes have received significant attention in recent years because of their importance in a wide range of applications that encompass industrial processes, catalysis and some organic transformations.[1–4] As a consequence, considerable effort has been devoted to studies of the structures, reactivities and bonding of this class of compound.[1–6] In the particular case of titanium imido complexes, heightened interest has stemmed from the idea that such compounds might serve as single-source precursors for the CVD (chemical vapour deposition) of titanium nitride (TiN). In turn, TiN has assumed an important role as a diffusion barrier in a variety of metallisation structures of advanced microelectronic devices due to its low resistivity, excellent thermal stability, and high tolerance to chemical etching.[7,8] In some cases, imido complexes of titanium have been proposed as intermediates in the conversion of other titanium–nitrogen derivatives into TiN. For example, the thermal reactions of homoleptic titanium amides, $Ti(NR_2)_4$, with ammonia vapour have been postulated to proceed *via* imido complexes of the type $[Ti(NH)(NR_2)_2]$ (R = Me or Et).[9] In other cases, stable titanium imido complexes have been isolated, characterised, and tested as potential single-source precursors to TiN. The list includes $[\{Ti(NBu^t)Cl_2(NH_2Bu^t)_2\}_3]$ **1**,[10] $[Ti(NBu^t)Cl_2(OPPh_3)_2]$ **2**,[11] $[Ti(NBu^t)Cl_2(TMEDA)]$ **3** (TMEDA = *N*,*N*,*N*′,*N*′-tetramethylethylenediamine),[10] $[Ti(NBu^t)Cl_2(DIPEDA)]$ **4** (DIPEDA = *N*,*N*′-diisopropylethylenediamine),[10] and $[Ti(NH)Cl_2(OPPh_3)_2]$ **5**.[12] Further examples include $Ti(NR_2)_4$ (R = Me or Et),[13] $[Ti(NMe_2)_3(Bu^t)]$,[13] $[Ti(\mu\text{-}NBu^t)(NMe_2)_2]_2$,[13] $[CpTiCl_2\{(N(SiMe_3)_2\}]$,[14] $[TiCp_2(N_3)_2]$,[15] $[TiCl_4(NH_3)_2]$,[16] and $[\{TiCl_2(NHBu^t)_2(NH_2Bu^t)_2\}_n]$.[11] However, despite the foregoing developments, a completely satisfactory TiN single-source precursor has yet to emerge. In some cases, precursor volatilities are unacceptably low due to dimerisation or higher degrees of oligomerisation. In other cases, it has been found that precursors with Ti–C bonds result in high levels of carbon contamination, while precursors with Ti–Cl bonds are potentially corrosive to metal substrates, such as steel or aluminium, at the temperatures at which CVD reactions are carried out.[16]

With a view to addressing some of the foregoing problems, we are developing TiN precursors with an all-nitrogen coordination sphere thus reducing the possibility of contamination from the species, such as C or Cl, in the resulting TiN films. In a previous publication[17] we described the synthesis and characterisation of precursors of the type $[Ti(NMe_2)_2(N_3)_2(py)_n]$ (n = 0 **6** or 2 **7**). In the present contribution we describe (a) a gas-phase pyrolysis study of **7**, and (b) the syntheses and structures of two novel imidoazido titanium(IV) complexes.

Results and Discussion

The reaction between $[Ti(NBu^t)Cl_2(NH_2Bu^t)_2]_3$ **1**[10] and 6 equivalents of Me_3SiN_3 in the presence of an excess of pyridine (py) at room temperature resulted, after work-up, in a 40% yield of orange crystalline **8** (Scheme 1). As outlined in Scheme 1, the addition of pyridine to compound **1** resulted initially in the formation of the intermediate $[Ti(NBu^t)Cl_2(py)_3]$ **9**, a compound which has been reported previously (but not isolated).[6,18] Analytical and spectroscopic data for **8** were consistent with the empirical composition $[\{Ti(NBu^t)Cl(N_3)(py)_2\}_2]$ rather than that of the anticipated product $[Ti(NBu^t)(N_3)_2(py)_3]$ **10**. However, in order to establish both the degree of oligomerisation and the stereochemistry at titanium, an X-ray crystallographic

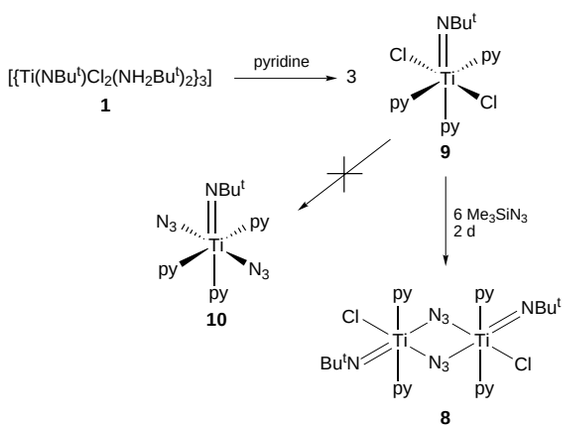

Scheme 1

† Current address: Department of Chemistry, University College London, 20 Gordon Street, London, UK WC1H 0AJ.

Table 1 Selected bond distances (Å) and angles (°) for compounds **8** and **11**

Compound **8**		Compound **11**	
Ti(1)–N(4)	1.689(4)	Ti(1)–N(7)	1.695(3)
Ti(1)–N(1)	2.140(4)	Ti(1)–N(4)	2.065(3)
Ti(1)–N(5)	2.246(4)	Ti(1)–N(1)	2.122(3)
Ti(1)–N(6)	2.235(4)	Ti(1)–N(8)	2.239(3)
Ti(1)–N(1a)	2.359(4)	Ti(1)–N(9)	2.242(3)
Ti(1)–Cl(6)	2.418(2)	Ti(1)–N(1a)	2.346(3)
N(4)–Ti(1)–N(1)	98.9(2)	N(7)–Ti(1)–N(4)	106.2(1)
N(4)–Ti(1)–N(5)	95.4(2)	N(7)–Ti(1)–N(1)	100.1(1)
N(1)–Ti(1)–N(5)	91.1(1)	N(4)–Ti(1)–N(1)	153.7(1)
N(4)–Ti(1)–N(6)	96.0(2)	N(7)–Ti(1)–N(8)	94.6(1)
N(1)–Ti(1)–N(6)	91.1(2)	N(4)–Ti(1)–N(8)	87.5(1)
N(5)–Ti(1)–N(6)	167.9(2)	N(1)–Ti(1)–N(8)	89.7(1)
N(4)–Ti(1)–N(1a)	169.8(2)	N(7)–Ti(1)–N(9)	93.3(1)
N(1)–Ti(1)–N(1a)	70.9(2)	N(4)–Ti(1)–N(9)	88.6(1)
N(5)–Ti(1)–N(1a)	84.1(1)	N(1)–Ti(1)–N(9)	90.7(1)
N(6)–Ti(1)–N(1a)	85.4(1)	N(8)–Ti(1)–N(9)	171.9(1)
N(4)–Ti(1)–Cl(1)	102.7(2)	N(7)–Ti(1)–N(1a)	170.1(1)
N(1)–Ti(1)–Cl(1)	158.5(1)	N(4)–Ti(1)–N(1a)	83.7(1)
N(5)–Ti(1)–Cl(1)	86.4(1)	N(1)–Ti(1)–N(1a)	70.0(1)
N(6)–Ti(1)–Cl(1)	87.2(1)	N(8)–Ti(1)–N(1a)	85.4(1)
N(1a)–Ti(1)–Cl(1)	87.5(1)	N(9a)–Ti(1)–N(1a)	87.1(1)
N(2)–N(1)–Ti(1)	123.2(3)	N(2)–N(1)–Ti(1)	124.8(2)
N(2)–N(1)–Ti(1a)	126.7(3)	N(2)–N(1)–Ti(1a)	125.2(2)
Ti(1)–N(1)–Ti(1a)	109.1(2)	Ti(1)–N(1)–Ti(1a)	109.97(1)
N(3)–N(2)–N(1)	179.0(5)	N(3)–N(2)–N(1)	178.5(4)

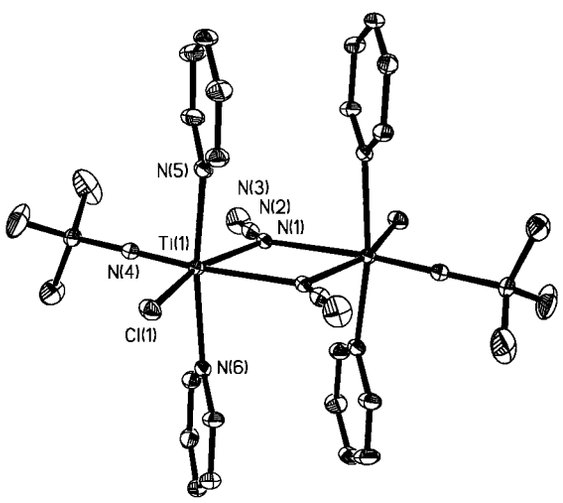

Fig. 1 View of the structure of compound **8** showing the atom numbering scheme. Ellipsoids are drawn at the 30% level. Hydrogen atoms are omitted for clarity. Only one component of the disorder affecting C(2), C(3) and C(4) is shown

study was carried out, the results of which are depicted in Fig. 1; selected bond lengths and angles are presented in Table 1. The crystal structure of **8** revealed that individual $[Ti(NBu^t)Cl(N_3)(py)_2]$ units are associated into centrosymmetric dimers *via* bridging azide interactions. Thus, the coordination number at each titanium centre is six and the geometry is approximately octahedral. The stereochemistry at titanium is such that one of the bridging azide groups is located *trans* to the *tert*-butylimido substituent while the other is *trans* to Cl(1); the two pyridine ligands also adopt a mutually *trans* arrangement. The Ti_2N_2 core is basically rhombohedral with the bond angle at nitrogen [109.1(2)°] being considerably larger than that at titanium [70.9(2)°]. However, the two Ti–N bond distances differ by $\Delta = 0.219$ Å [Ti(1)–N(1) 2.140(4), Ti(1)–N(1a) 2.359(4) Å] suggesting that the dimers are somewhat weakly bonded. This type of bridge asymmetry is also evident in $[\{Ti(C_5H_4Me)Cl_2N_3\}_2]$, but in this case Δ is considerably smaller (0.027 Å).[19] Another noteworthy structural feature is that the average Ti–N bond distance for the Ti_2N_2 core of **8** [2.245(4) Å] is considerably longer than those in $[\{Ti(C_5H_4Me)Cl_2N_3\}_2]$[19] (average 2.134 Å), $[TiCl_3(N_3)]$[20] (average Ti–N_3 2.105 Å), and $[AsPh_4]_2[TiCl_4(N_3)]_2$[21] (average Ti–$N_3$ 2.116 Å), again suggesting somewhat weaker dimerisation. As expected, the Ti–N (azide) bond distances in **8** are longer than those in compounds which feature terminal azide ligands, namely $[Ti(NMe_2)_2(N_3)_2(py)_2]$ [2.075(5) Å],[17] $[Ti(NMe_2)_2(N_3)_2(bipy)]$ (bipy = 2,2′-bipyridyl) [2.067(5) Å],[17] $[Ti(NMe_2)_3(N_3)(bipy)]$ [2.150(5) Å],[17] $[Ti(C_5H_5)_2(N_3)_2]$[22] (average Ti–N_3 2.03 Å) and $[AsPh_4]_2[TiCl_4(N_3)_2]$[23] (average Ti–$N_3$ 2.01 Å). The titanium–imido moieties are essentially linear [Ti(1)–N(4)–C(1) 177.0(4)°] and thus consistent with donation of the lone pair on nitrogen into an acceptor orbital on titanium. The Ti=N bond distance in **8** [1.689(4) Å] is considerably shorter than those in some related monomeric titanium imido complexes of the type $[Ti(NR)Cl_2L_n]$ [$n = 3$, L = py, R = Bu^t, Ph, C_6H_4Me–4, C_6H_4-NO_2–4, P(S)Ph_2 or P(S)Pr^i_2; $n = 2$, L = 4-*tert*-butylpyridine, R = Bu^t; $n = 1$, L = TMEDA, R = Ph] which span the range of 1.705(3)–1.723(2) Å.[6,18,24–27] However, it is longer than those found in **2** [1.672(8) Å][11] and **4** [1.681(7) Å].[10] The observation that complexes **3** and **5** have much shorter Ti=N bond distances [1.662(4) and 1.627(8) Å, respectively] is attributable to the modest steric demands of the hydrogen substituent in the latter compound.[11,12] The reason for the range of Ti=N bond lengths observed for **8** and related complexes is not completely clear; however, in general it has been observed that the Ti=N bond distances of arylimido derivatives are longer than those of *tert*-butylimido analogues.[6] The Ti–Cl [2.418(2) Å] and the Ti–N(py) [average 2.241(5) Å] bond distances in **8** are similar to those in **9** but longer than the corresponding values observed in arylimido derivatives. This labilising effect of the *tert*-butylimido ligand has been observed previously in complexes of the type $[Ti(NR)Cl_2L_n]$ (see above).[6] Commenting more generally on the structure of **8**, it is interesting that the related dichloride complexes of the type $[Ti(NR)Cl_2L_n]$ are all monomeric in the solid state.[6,10–12,18,24–27] Also interesting is that in **8** it is the azides rather than the chloride ligands that adopt bridging positions. Such a preferential bridge bonding of azide *versus* chloride ligands is also evident in $[AsPh_4]_2[TiCl_4(N_3)_2]$.[23]

In concert with the presence of potentially corrosive chloride ligands, the diminished volatility of complex **8** due to dimerisation render it unattractive as a potential TiN source. With a view to developing a monomeric species with an all-nitrogen coordination sphere, it was decided to attempt the reaction of $[Ti(NMe_2)_2(N_3)_2(py)_2]$ **7**[17] with an alkylamine. The reaction of **7** with 1 equivalent of $CyNH_2$ (Cy = cyclohexyl) in the presence of an excess of pyridine at room temperature resulted in a 70% yield of an orange crystalline product after work-up and recrystallisation from CH_2Cl_2 (Scheme 2). Analytical and spectroscopic data were consonant with the formulation $[\{Ti(NCy)(N_3)_2(py)_2\}_2]$ **11**. The dimeric nature of **11** was confirmed by a subsequent X-ray crystallographic study, the results of which are depicted in Fig. 2; selected bond lengths and angles are

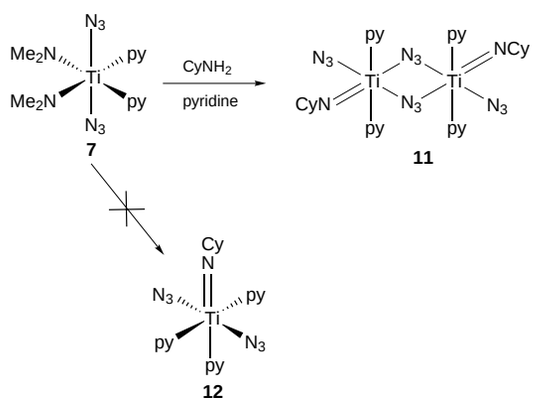

Scheme 2

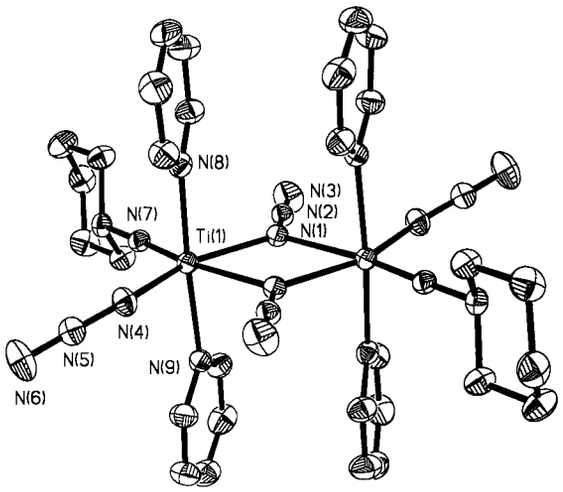

Fig. 2 View of the structure of compound **11** showing the atom numbering scheme. Ellipsoids are drawn at the 30% level. Hydrogen atoms are omitted for clarity

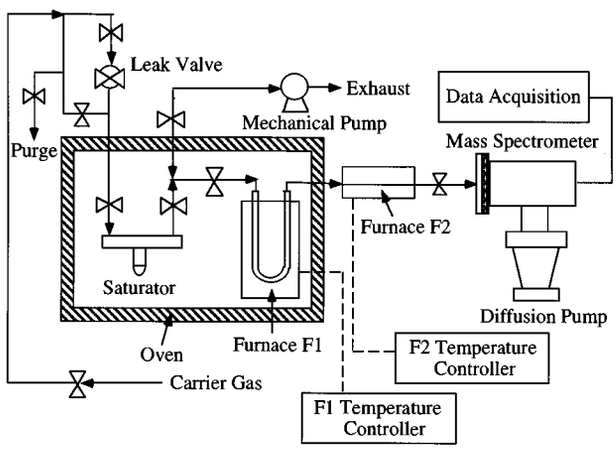

Fig. 3 Gas-phase pyrolysis system

presented in Table 1. The molecular structure of **11** is similar to that of **8** in the sense that monomeric units are associated into centrosymmetric dimers *via* somewhat asymmetric azide bridging interactions [Ti(1)–N(1) 2.122(3), Ti(1)–N(1a) 2.346(3) Å]. The geometry at the titanium centre in **11** is approximately octahedral and similar to that in **8** but with a chloride replaced by a terminal azide ligand, *viz*. the pyridine ligands are arranged in a mutually *trans* fashion, while the terminal azide ligand and cyclohexylimido ligands adopt a *cis* relationship with respect to each other. The two remaining *cis* sites are occupied by the bridging azido ligands. The Ti=N and Ti–N(py) bond lengths in **11** [1.695(3) and 2.241(3) Å (average), respectively] are identical to those in **8** within experimental error, hence the discussion of these aspects presented above for **8** is also valid for **11**. The terminal Ti–N_3 bond distance of 2.065(3) Å in **11** is similar to that in the precursor complex **7** [2.075(5) Å][17] as well as those in other titanium complexes with terminal azide ligands.[17,22,23] Another noteworthy point is that the angles subtended at titanium between the imido nitrogen and the atoms *cis* to it are all greater than 90°, presumably due to the enhanced bond pair–bond pair repulsions on account of the double bond. This effect has been observed by others.[6] Finally, attention is drawn to the fact that replacement of two chloride ligands in previously reported complexes of the type $[Ti(NR)Cl_2(py)_3]$[6,18,24–26] by azide ligands results in azide bridge bonding rather than completion of the co-ordination sphere by addition of a third pyridine ligand.

Unfortunately, the low volatility of complex **11** precluded thin film growth. However, we have previously reported the deposition of TiN films using **7** as the single-source precursor.[17]

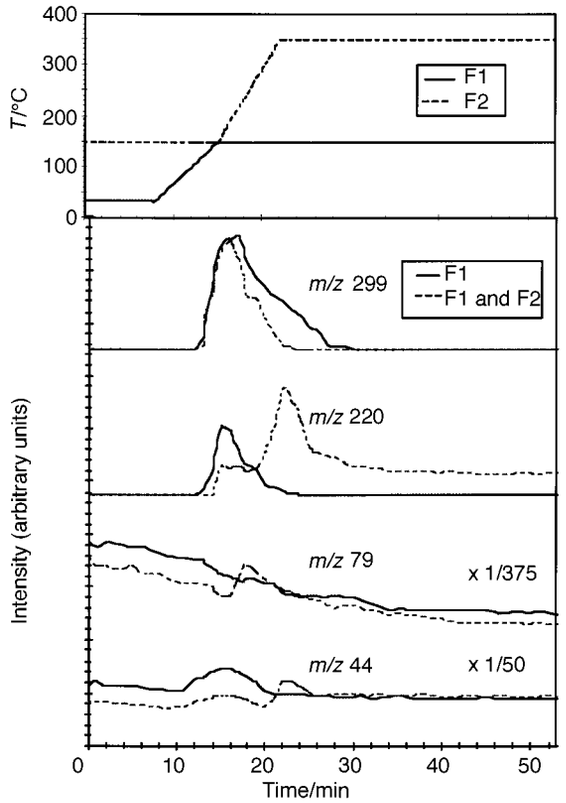

Fig. 4 Gas-phase pyrolysis of compound **7** showing the mass spectral fragments having *m/z* 299, 220, 79 and 44

We were therefore interested in gaining additional insights into the mechanism of the conversion of **7** into TiN. Accordingly, a gas-phase pyrolysis study of **7** was conducted in a slightly modified version (Fig. 3) of an apparatus described previously.[28] The major update involved the addition of a second furnace (F2) to the one present in the original design (F1). The modified system has a base pressure of 3×10^{-7} Torr (*ca.* 4×10^{-5} Pa). This modification permitted flashing of the precursor **7** (which condenses at 35 °C) from the section of quartz tubing inside F1 followed by pyrolysis of this flashed amount in a section of stainless-steel tubing inside F2. This arrangement was necessary because the sublimation vapour pressure of **7** in the temperature range 35–90 °C was too low to permit the detection of titanium-bearing ions in the mass spectrometer. The results of two different experiments are summarised in Fig. 4. The solid curves, designated F1, are representative ion signals when **7** was flashed at 150 °C but not pyrolysed. Note the presence of large background signals at *m/z* 79 (py^+), 44 (NMe_2^+) and 28 (N_2^+) when **7** undergoes sublimation in the system. Nevertheless, the presence of the anticipated signals corresponding to $[Ti(NMe_2)_2(N_3)_2(py)]^+$ (*m/z* 299), $[Ti(NMe_2)_2(N_3)_2]^+$ (*m/z* 220) and $[Ti(NMe_2)_2(py)]^+$ (*m/z* 215) and $[Ti(NMe_2)_2]^+$ (*m/z* 136) (not shown in Fig. 4) suggests that **7** transports intact. The curves designated F1 and F2 are representative ion signals that were detected when **7** was flashed at 150 °C and subsequently pyrolysed in furnace section F2. The change in the $[Ti(NMe_2)_2(N_3)_2(py)]^+$ (*m/z* 299) signal profile relative to F1 at ≈180 °C and the appearance of a $[py]^+$ signal (*m/z* 79) above the background at ≈180 °C indicates that the initial thermolytic step is cleavage of the Ti–N (py) bonds (Scheme 3). In turn, the loss of pyridine ligands leads to the formation of $[Ti(NMe_2)_2(N_3)_2]$ **6**, which may have a different ionisation cross-section than that of **7**. The leading edge of the *m/z* 220 peak for F1 and F2 corresponds to the presence of intact **7**. It is interesting that the *m/z* 220 signal increases at a higher F2 temperature than does the *m/z* 79 signal. Compound **6** has a much lower vapour pressure than **7**[17] hence the former could be condensing on the tube walls in F2 and thus could be flashed off as the F2 tem-

$$\mathrm{Ti(NMe_2)_2(N_3)_2(py)_2}$$
$$\downarrow \approx 180\ ^\circ\mathrm{C}$$
$$\mathrm{Ti(NMe_2)_2(N_3)} + \mathrm{[py]}$$
$$\downarrow \approx 290\ ^\circ\mathrm{C}$$
$$\mathrm{Ti(NMe_2)_2(N_3)} + \mathrm{[NMe_2]} + \mathrm{[N_2]} + \mathrm{TiN}$$

Scheme 3 Proposed reaction steps for decomposition of compound **7**

perature increases to ≈260 °C. Unfortunately, the large background signal for $[N_2]^+$ (*m*/*z* 28) precludes any discussion of azide ligand decomposition. However, an increase in the $[NMe_2]^+$ (*m*/*z* 44) peak intensity at ≈292 °C indicates that cleavage of the Ti–NMe_2 bond is the next step in the decomposition pathway (Scheme 3). In turn, this might suggest that the amido ligands desorb intact during the film-growth study of **7** at 350 °C and that the azide ligand is the nitrogen source for the TiN films.

In conclusion, the pyrolysis study of compound **7** shows that it can be sublimed intact but has a low vapour pressure. The pyridine ligand assists in the vapour transport of the precursor; however, there is no evidence that it enters into the thermolysis process hence it should not contaminate the resulting TiN films.

Experimental

General procedures

All manipulations were performed under a dry, oxygen-free dinitrogen or argon atmosphere using standard Schlenk techniques or in a HE-493 Vacuum Atmosphere dry-box. Unless otherwise stated, all solvents were dried over sodium and distilled from sodium–benzophenone under argon prior to use. Trimethylsilyl azide and cyclohexylamine were dried over molecules sieves. The authors are grateful to Advanced Delivery & Chemical Systems, Inc. for a sample of $Ti(NMe_2)_4$ which was used without further purification. All other reagents were procured commercially and used without further purification. Elemental analyses were performed by Atlantic Microlab, Inc., Norcross, GA.

Physical measurements

Mass spectra (CI) were run on a MAT 4023 instrument, and NMR spectra were recorded on a GE QE-300 spectrometer (^{1}H, 300.19 MHz; ^{13}C, 75.48 MHz). The NMR spectra are referenced to CD_2Cl_2 which was dried over sodium–potassium alloy and distilled prior to use; ^{1}H and ^{13}C chemical shifts are reported relative to $SiMe_4$ (0.00 ppm). Melting points were obtained in sealed glass capillaries under argon and are uncorrected.

Preparations

Compound 8. The compound Me_3SiN_3 (1.2 cm^3, 8.87 mmol) was added dropwise to a orange-red solution of $[\{Ti(NBu^t)Cl_2(NH_2Bu^t)_2\}_3]$[10] (1.49 g, 1.48 mmol) in pyridine (40 cm^3) at room temperature. The solution turned blood red after a few minutes and was allowed to stir for 2 d, after which time the solvent was removed *in vacuo*. The resulting red solid was redissolved in CH_2Cl_2 (8 cm^3) to give an orange solution. Cooling of this solution to −20 °C overnight afforded a 40% yield of orange crystalline **8** (m.p. 120–122 °C). ^{1}H NMR (300.15 MHz, CD_2Cl_2): δ 0.94 (s, 18 H, NBu^t), 7.16 (br, 8 H, *m*-H of C_5H_5N), 7.71 (br, 4 H, *p*-H of C_5H_5N) and 8.67 (br, 8 H, *o*-H of C_5H_5N), ^{13}C-{^{1}H} NMR (75.14 MHz, CD_2Cl_2): δ 29.6 [$NC(CH_3)_3$], 70.4 [$NC(CH_3)_3$], 124.6 (*m*-C of C_5H_5N), 137.9 (*p*-C of C_5H_5N) and 151.8 (*o*-C of C_5H_5N). FTIR: 2079.5 cm^{-1} (N_3) (Found: C, 47.72; H, 5.03; N, 23.84. Calc. for $C_{14}H_{19}ClN_6Ti$: C, 47.41; H, 5.39; N, 23.69%).

Compound 11. The dropwise addition of $CyNH_2$ (0.5 cm^3, 4.28 mmol) to a blood-red solution of $[Ti(NMe_2)_2(N_3)_2(py)_2]$[17] (1.62 g, 4.28 mmol) in pyridine (40 cm^3) at room temperature resulted in a change to orange. The reaction mixture was allowed to stir for 2 d, after which the solvent was removed *in vacuo*. The resulting orange solid was redissolved in CH_2Cl_2 (8 cm^3) to give an orange solution. Cooling of this solution to −20 °C overnight afforded a 70% yield of orange crystalline **11** (m.p. 112–114 °C). ^{1}H NMR (300.15 MHz, CD_2Cl_2): δ 0.839–1.820 (m, 22 H, NCy), 7.27 (t, J = 7.8, 8 H, *m*-H of C_5H_5N), 7.67 (t, J = 7.8, 4 H, *p*-H of C_5H_5N) and 8.58 (d, J 7.8 Hz, 8 H, *o*-H of C_5H_5N), ^{13}C-{^{1}H} NMR (75.14 MHz, CD_2Cl_2); δ 25.2, 26.1, 35.3, 76.5 (NCy), 124.6 (*m*-C of C_5H_5N), 136.8 (*p*-C of C_5H_5N) and 150.3 (*o*-C of C_5H_5N). FTIR: 2069.4 cm^{-1} (N_3) (Found: C, 49.81; H, 5.16; N, 31.89. Calc. for $C_{16}H_{21}N_9Ti$: C, 49.62; H, 5.47; N, 32.55%).

Table 2 Crystal data, details of intensity, measurement, and structure refinement for compounds **8** and **11**

	8	**11**
Formula	$C_{28}H_{38}Cl_2N_{12}Ti_2\cdot 2CH_2Cl_2$	$C_{16}H_{21}N_9Ti\cdot CH_2Cl_2$
M	951.32	472.24
Crystal system	Rhombohedral	Monoclinic
Space group	$R\bar{3}$	$P2_1/c$
a/Å	33.919(8)	9.943(1)
b/Å	33.919(8)	12.329(1)
c/Å	10.857(2)	18.593(2)
β/°		104.024(8)
U/Å^3	10 818(4)	2211.2(4)
Z	9	4
D_c/g cm^{-3}	1.314	1.419
μ/cm^{-1}	7.04	6.52
Crystal size/mm	0.6 × 0.3 × 0.3	0.75 × 0.38 × 0.31
θ Range/°	2.08 to 25.00	2.68 to 24.97
Total no. reflections	5361	5064
No. observed reflections	4232	3879
No. refined parameters	266	265
Goodness of fit on F^2	1.041	1.046
$wR2$, $R1$* [$I(2\sigma)<I$]	0.2451, 0.0765	0.1401, 0.0500

* $R1 = \Sigma||F_o|-|F_c||/\Sigma|F_o|$, $wR2 = [\Sigma w(F_o^2 - F_c^2)^2/\Sigma w(F_o^2)^2]^{\frac{1}{2}}$, $w = 1/[\sigma^2(F_o^2) + (aP)^2 + bP]$ where $P = [\max(0,F_o^2) + 2F_c^2]/3$.

X-Ray crystallography

Crystals of compounds **8** and **11** were grown from CH_2Cl_2 solutions stored at −20 °C. The data set for **8** was collected on a Siemens P4 diffractometer at −100 °C, and an Enraf-Nonius CAD4 diffractometer was used for the collection of data for **11** at 25 °C. Graphite-monochromated Mo-Kα radiation (λ = 0.71073 Å) was used for both structures. Accurate unit-cell parameters were determined by recentering 25 optimum high-angle reflections. Three standard reflections were measured every 1800 s during data collection, and no decrease in intensities was noted. Corrections were applied for Lorentz-polarisation and absorption (for **8** only) effects. Both structures were solved by direct methods. The methyl carbon atoms, C(2), C(3) and C(4), of **8** were refined with large and highly anisotropic displacement parameters. It was determined that a disordered model was appropriate. These atoms were first refined isotropically. Large peaks on either side of these atoms were observed in a ΔF map. These six peak positions were used as starting points for a disordered model. The site occupancy factor for the two orientations of the *tert*-butyl group was refined while refining a common isotropic displacement parameter for all six atoms. This refinement indicated that the two orientations should be assigned equal weight. Therefore the atoms were assigned an occupancy factor of one-half and refined with isotropic displacement parameters. The C–C bond angles of this group were restrained to be approximately equal. However, no restrictions were placed on the bond lengths. The atoms were refined anisotropically with U_{ij} restrained to be approximately isotropic. In

the region of the $\bar{3}$ site symmetry there appeared three peaks from a badly disordered solvent molecule. All attempts to fit a chemically sensible CH_2Cl_2 molecule to these peaks were unsatisfactory. The electron density in this region was accounted for by assigning each peak as a carbon atom and refining with isotropic displacement parameters. Subsequent difference syntheses gave all other non-hydrogen atomic positions and these were refined by full-matrix least squares on F^2 using the Siemens SHELXTL PLUS software package.[29] All non-hydrogen atoms were allowed anisotropic thermal motion. The hydrogen atoms were included at calculated positions (C–H 0.96 Å) and refined using a riding model. Crystallographic data and details of the data collection procedures and structure refinement for **8** and **11** are presented in Table 2.

CCDC reference number 186/817.

Acknowledgements

Dr. Vincent Lynch of the departmental crystallography laboratory at The University of Texas at Austin is thanked for the low-temperature data collection for compound **8**. We are grateful to the Science and Technology Center Program of the National Science Foundation (CHE-08920120), the National Science Foundation (CHE-9629088), and the Robert A. Welch Foundation for generous financial support.

References

1 D. E. Wigley, *Prog. Inorg. Chem.*, 1994, **42**, 239.
2 W. A. Nugent and J. M. Mayer, *Metal–Ligand Multiple Bonds*, Wiley-Interscience, New York, 1988.
3 W. A. Nugent and B. L. Haymore, *Coord. Chem. Rev.*, 1969, **8**, 709.
4 V. C. Gibson, *Adv. Mater.*, 1994, **6**, 37.
5 D. C. Bradley, *Chem. Rev.*, 1989, **30**, 1962.
6 A. J. Blake, P. E. Collier, S. C. Dunn, W.-S. Li, P. Mountford and O. V. Shishkin, *J. Chem. Soc.*, *Dalton Trans.*, 1997, 1549.
7 S. T. Oyama, *The Chemistry of Transition Metal Carbides and Nitrides*, Blackie Academic & Professional, Glasgow, 1996.
8 H. B. Pogger, *Electronic Materials Chemistry*, Marcel Dekker, New York, 1996 and refs. therein.
9 R. M. Fix, R. G. Gordon and D. M. Hoffman, *J. Am. Chem. Soc.*, 1990, **112**, 7833; *Chem. Mater.*, 1991, **3**, 1138; see also, D. M. Hoffman, *Polyhedron*, 1994, **13**, 1169.
10 T. S. Lewkebandara, P. H. Sheridan, M. J. Heeg, A. L. Rheingold and C. H. Winter, *Inorg. Chem.*, 1994, **33**, 5879.
11 C. H. Winter, P. H. Sheridan, T. S. Lewkebandara, M. J. Heeg and J. W. Proscia, *J. Am. Chem. Soc.*, 1992, **114**, 1095.
12 P. J. McKarns, G. P. A. Yap, A. L. Rheingold and C. H. Winter, *Inorg. Chem.*, 1996, **35**, 5968.
13 R. M. Fix, R. G. Gordon and D. M. Hoffman, *Chem. Mater.*, 1990, **2**, 235 and refs. therein.
14 R. Laurent, J. S. Zhao, L. Valade, R. Choukroun and P. Cassoux, *J. Anal. Appl. Pyrolysis*, 1992, **24**, 39.
15 K. Ikeda, M. Maeda and Y. Arita, *Jpn. J. Appl. Phys.*, 1993, **32**, 3085.
16 C. H. Winter, T. S. Lewkebandara, J. W. Proscia and A. L. Rheingold, *Inorg. Chem.*, 1994, **33**, 1227.
17 C. J. Carmalt, A. H. Cowley, R. D. Culp, R. A. Jones, Y.-M. Sun, B. Fitts, S. Whaley and H. W. Roesky, *Inorg. Chem.*, 1997, **36**, 3108.
18 P. E. Collier, S. C. Dunn, P. Mountford, O. V. Shishkin and D. Swallow, *J. Chem. Soc.*, *Dalton Trans.*, 1995, 3743.
19 K. Kirschbaum and D. M. Giolando, *Acta Crystallogr.*, *Sect. C*, 1992, **48**, 1837.
20 H.-O. Wellern and U. Müller, *Chem. Ber.*, 1976, **109**, 3039.
21 U. Müller, W.-M. Dyck and K. Dehnicke, *Z. Anorg. Allg. Chem.*, 1980, **468**, 172.
22 E. R. De Gil, M. De Burguera, A. v. Rivera and P. Maxfield, *Acta Crystallogr.*, *Sect. B*, 1977, **33**, 578.
23 W.-M. Dyck, K. Dehnicke, F. Weller and U. Müller, *Z. Anorg. Allg. Chem.*, 1980, **470**, 89.
24 H. W. Roesky, H. Voelker, M. Witt and N. Noltemeyer, *Angew. Chem.*, *Int. Ed. Engl.*, 1990, **29**, 669.
25 H. W. Roesky, T. Raubold, M. Witt, R. Bohra and N. Noltemeyer, *Chem. Ber.*, 1991, **124**, 1521.
26 S. C. Dunn, A. S. Batsanov and P. Mountford, *J. Chem. Soc.*, *Chem. Commun.*, 1994, 2007.
27 R. Duchateau, A. J. Williams, S. Gambarotta and M. Y. Chiang, *Inorg. Chem.*, 1991, **30**, 4863.
28 J. E. Miller, M. A. Mardones, J. W. Nail, A. H. Cowley, R. A. Jones and J. G. Ekerdt, *Chem. Mater.*, 1992, **4**, 447; J. E. Miller and J. G. Ekerdt, *Chem. Mater.*, 1992, **4**, 7.
29 G. M. Sheldrick, SHELXTL PLUS PC, Version 5.0, Siemens Analytical X-Ray Instruments, Inc., Madison, WI, 1994.

Received 22*nd July* 1997; *Paper* 7/05246D